

# THE BEHAVIOR, STABILITY PROPERTIES, AND POTENTIAL APPLICATIONS OF RHAMNOLIPID BIOSURFACTANTS IN OIL DEGRADATION

Muhamad Hissammuddin Shah Zainal Abidin<sup>a,b</sup>, Nor Dina Sakaria<sup>a,b</sup>, Nur Raudhah Azman<sup>a,c</sup>, Umi Aisah Asli<sup>a\*</sup>

<sup>a</sup>Chemical Reaction Engineering Group (CREG), Faculty of Chemical and Energy Engineering, Faculty of Engineering, Universiti Teknologi Malaysia, Johor Bahru, 81310 UTM Johor Bahru, Johor, Malaysia

<sup>b</sup>Politeknik Tun Syed Nasir Syed Ismail (PTSNI), Pagoh Educational Hub, Pagoh, 84600 Johor, Malaysia

<sup>c</sup>Innovation Center in Agritechology for Advanced Bioprocessing (ICA), UTM Pagoh Campus, Pagoh Educational Hub, Pagoh, 84600 Johor, Malaysia

## Article history

Received

19 August 2022

Received in revised form

05 July 2023

Accepted

13 July 2023

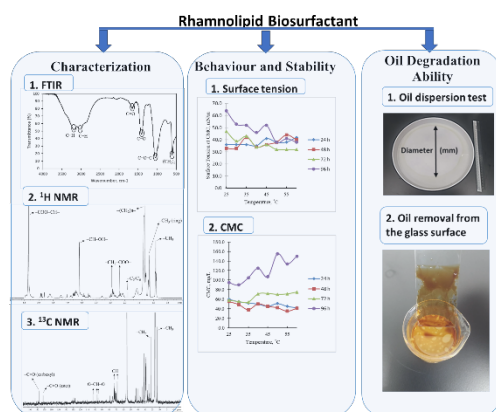
Published online

30 November 2023

\*Corresponding author

umi\_aisyah@utm.my

## Graphical abstract



## Abstract

Rhamnolipid biosurfactants are among the most investigated for various applications, owing not only to their much lower environmental impact compared to chemical surfactants but also because they have proven effective in reducing surface tension and critical micelle concentration (CMC). However, there is concern regarding their high cost. This work aims to determine important behavior and properties of rhamnolipids and verify their potential for oil degradation. They were characterized using FTIR, <sup>1</sup>H NMR, and <sup>13</sup>C NMR spectroscopy to determine the main functional groups and the chemical structure of rhamnolipids for oil degreasing. Then, the influence of thermodynamic properties on CMC stability was studied to establish the stability behavior. This investigation is essential as good oil degreasing products require low CMC values to minimize the amount used during the oil removal process, form micelles, and solubilize dirt and oil. The oil degradation ability of rhamnolipids in different concentrations was studied using an oil dispersion test and the method of oil removal from a glass surface. Overall, this investigation proves that the temperature of the solution and immersion time influenced the CMC and surface tension value for the rhamnolipids. The lowest CMC value was 35 mg/L at 55 °C after 48 h of stabilization. The minimum recommended amount of rhamnolipids for the oil degrease formulation was also found to be 0.1% w/v, which is very low. This study showed that the behavior and stability of rhamnolipids are suitable for oil degradation applications and can efficiently replace chemical surfactants in oil degradation products.

**Keywords:** Stability properties, characterization, critical micelle concentration, rhamnolipid biosurfactant, oil degradation

© 2023 Penerbit UTM Press. All rights reserved

## 1.0 INTRODUCTION

Heavy oil pollution is extremely hazardous and irrevocably damaging to the environment. The study of environmental cleaning and restoration practices is crucial to prevent the poisoning and death of living organisms due to this pollution. The pervasive early use of synthetic materials for oil degradation caused the water to be more toxic than the oil [1]. Various oil

degradation methods exist, including solvent extraction and chemical dispersion [2]. However, these methods do not completely eliminate hydrocarbon contaminants from the environment and potentially can lead to water source contamination [2].

A previous study has shown that biosurfactants can be an alternative to other methods with tremendous potential for oil degradation [3], [4]. Biosurfactants are better than chemical

surfactants due to their ecological properties, especially their reduced toxicity and enhanced biodegradability [5]. In addition, biosurfactants are highly efficient at emulsifying hydrophobic hydrocarbons, that is, increasing their solubility in water and decreasing surface tension, which are crucial for oil degradation [6].

Biosurfactants are classified by organism source, molecular weight, and chemical structure [7]–[9]. Low molecular weight biosurfactants, which are mostly glycolipids, lipopeptides and lipoproteins, fatty acids, neutral lipids, and phospholipids, are more effective and very efficient in lowering the surface and interfacial tensions. In contrast, high molecular weight biosurfactants, such as polymeric and particulate biosurfactants, are more efficient as emulsion-stabilizing agents [10]–[12].

Rhamnolipids are anionic glycolipid biosurfactants with amphiphilic characteristics typically isolated from *Pseudomonas aeruginosa* [13]. Numerous studies have investigated the benefits of rhamnolipids, which have become the most popular category of biosurfactant. Rhamnolipids are often considered the best bacterial surfactants due to their excellent physicochemical properties [7]. Furthermore, rhamnolipids can reduce the surface tension and critical micelle concentration (CMC) [14], [15]. The lowest surface tension and CMC values of rhamnolipids are within the ranges of 26–32 mN/m and 10–150 mg/L, respectively [13], [16]–[22].

One of the most significant characteristics of rhamnolipids is the ability to aggregate two different immiscible solutions. The CMC occurs at the minimum biosurfactant concentration, where surfactant monomers start to aggregate, forming micelles. The CMC is essential and crucial because it determines the efficacy of a surfactant and provides guidance on the limits of surfactant concentrations for specific uses [23], [24]. The lower the CMC, the less surfactant is required to emulsify, solubilize, and disperse oil effectively [25]. For example, cleaning products require low CMCs to minimize the amount used during cleaning, form micelles, and solubilize dirt and oil [26]. In other words, low CMC values can improve detergency properties, which are critical in applications such as cleaning products [27].

Theoretically, micelles will form when rhamnolipids are dissolved in water; the hydrophilic heads (i.e., rhamnose molecules) make contact with the water, and the hydrophobic tails (i.e., fatty acid chains) are sheltered inside [28]. Apart from the interactions of the head group, other factors also affect aggregation, including temperature, hydrogen bonding, van der Waals forces, and interactions between electrostatic forces [28]. The temperature significantly influences micellization, primarily because the head and tail group contacts change due to temperature changes. Previous research has empirically demonstrated that the CMC in anionic, cationic, and non-ionic surfactants is significantly affected by temperature [29], [30]. Early investigations of some anionic, cationic, and non-ionic surfactants under increasing temperatures have shown a decrease in CMC to a minimum point, and a subsequent increase, following a U-shaped pattern [31]. The CMC of cationic surfactants is typically greater than that of anionic surfactants having the same alkyl chain length [32].

The CMC of the surfactant influences the Gibbs free energy of micellization [30]. However, the CMC is the minimum concentration of surfactants that causes the aggregates to be thermodynamically soluble [24], [28]. Three critical values of thermodynamic properties, the (i) standard Gibbs energy of micellization,  $\Delta G^{\circ}_m$ ; (ii) entropy,  $\Delta S^{\circ}_m$ ; and (iii) enthalpy,  $\Delta H^{\circ}_m$ ,

are commonly determined [33]. To improve the understanding of these thermodynamic parameters, the effects of changes in time and temperature on the surface tension of biosurfactant (rhamnolipid) solutions at a wide range of concentrations require further investigation.

Numerous studies have been published on the effectiveness of cleaning by rhamnolipids, and their efficacy related to the cleaning process has been confirmed. For example, many studies on the use of rhamnolipids in the formulation of detergents have yielded intriguing results [15], [34], [35]. Additionally, rhamnolipids are effective for cleansing ultrafiltration membranes [36], [37] and whiteboards [38]. However, this study focuses on the stability properties of surface tension related to temperature that have rarely been studied. Due to their ability to reduce the water surface tension to a very low value, rhamnolipids have significant potential for applications in oil degradation.

Hence, this article aims to clarify the presence of functional groups and the chemical structure of rhamnolipids using Fourier transform infrared (FTIR),  $^1\text{H}$  NMR, and  $^{13}\text{C}$  NMR spectroscopy. Then, the stability of the surface tension and the CMC of rhamnolipids was studied at varying times and temperatures. Next, the potential of rhamnolipid for oil degradation was evaluated. This establishes baseline knowledge of whether rhamnolipids have the potential to replace chemical surfactants, particularly in oil degradation products, because chemical surfactants are potentially toxic, difficult to degrade in wastewater treatment, and have a detrimental effect on the environment [39], [40].

## 2.0 METHODOLOGY

### 2.1 Raw Material

The commercial rhamnolipid mixture R90 (90% purity, CAS No. 869062–42–0) was purchased from Sigma-Aldrich. The rhamnolipids was purified from *Pseudomonas aeruginosa* and contain varying length tails of fatty acid. The rhamnolipid mixture was used without further purification.

### 2.2 Physicochemical Characterization of Rhamnolipid Biosurfactants

The Rhamnolipids used were identified under the Glycolipid groups. The specific functional groups and chemical bonds of the rhamnolipid mixture were further analyzed using an iS5 FTIR spectrometer (Thermo Scientific Nicolet, USA). About 2 mg of the rhamnolipid powder was compressed into a thin pellet and examined in the 4000–400  $\text{cm}^{-1}$  region at a spectral resolution of 4  $\text{cm}^{-1}$  [41]. The structure of the rhamnolipid was characterized using an NMR spectrometer (400 MHz Bruker Avance III, Switzerland).  $^1\text{H}$  NMR and  $^{13}\text{C}$  NMR spectra were examined in this study. Rhamnolipid powder (3 to 4 mg) was dissolved in deuterated ethanol and analyzed [42]. Chemical shifts are shown in parts per million (ppm) and coupling constants in hertz (Hz).

## 2.3 Stability of the Rhamnolipid Biosurfactant

### 2.3.1 Surface Tension and CMC Determination

The surface tension of the rhamnolipid solution was determined by the capillary-rise method using a tensiometer (Cole-Parmer, USA) [43]. Rhamnolipid solutions at various aqueous concentrations were prepared and mixed thoroughly using a digital overhead stirrer (Cole-Parmer, USA) at 100 rpm for 2 min. To determine the surface tension values at various temperatures, 50 ml of each concentration of the aqueous rhamnolipid mixture was placed into a beaker in a Gyromax 939 XL incubator shaker (Amerex Instruments, Concord, CA, USA). The temperature of each solution was checked using a thermometer before the surface tension was measured.

The CMC was determined by plotting the surface tension (mN/m) versus concentration (mg/L), with the CMC value computed from the sharp breaks in the plotted data. Each solution was left to stabilize for 24 h and then analyzed every 24 h until 96 h had passed. Each experiment was conducted in triplicate.

### 2.3.2 Thermodynamic Properties

To compute the enthalpy of micellization ( $\Delta H_m^\circ$ ), the CMC was first calculated using a least-squares regression model [44]. Then, as described in Equation 1, a third-order polynomial equation was used to relate the CMC and the temperature and determine the coefficients a, b, c, and d. T is the absolute temperature (K).

$$\ln X_{\text{cmc}}(T) = a + bT + cT^2 + dT^3 \quad (1)$$

Next, by applying the Gibbs–Helmholtz equation, as shown in Equation 2, the enthalpy of micellization values, ( $\Delta H_m^\circ$ ) (Equation 3), were calculated by substituting Equation 1 into Equation 2, where R is the gas constant (8.314 J/mol·K).

$$\Delta H_m^\circ = -RT^2 \frac{d(G_m^0/T)}{dT} \quad (2)$$

$$\Delta H_m^\circ = \Delta G_m^\circ + T\Delta S_m^\circ \quad (3)$$

After the values for the enthalpy of micellization were obtained, the Gibbs free energy ( $\Delta G_m^\circ$ ) and entropy of micellization ( $\Delta S_m^\circ$ ) were determined using Equations 4 and 5.

$$\Delta G_m^\circ = RT \ln X_{\text{cmc}} \quad (4)$$

$$\Delta S_m^\circ = - \frac{1}{T(\Delta H_m^0 - \Delta G_m^0)} \quad (5)$$

## 2.4 Oil Degradation Ability of the Rhamnolipid Biosurfactant

### 2.4.1 Oil Displacement Test Method

The dispersion capacity of the rhamnolipid solution was determined using an oil displacement test (ODT). Saltwater was used to evaluate the effectiveness of oil spill surface tension reduction [45]. For this study, 250 mL of saltwater was poured into a 300-cm diameter round tray, followed by a drop of used

motor oil slowly added to the surface. Then, the rhamnolipid solution was poured into the round tray. The ratio of used motor oil to rhamnolipid solution was 1:1. Distilled water was used as a control. The experiment was conducted at room temperature, and the mean diameter of each clear zone was calculated [45], [46]. Figure 1 shows an example determination of the diameter of the dispersion region.



Figure 1 Determining the diameter of a clear zone formed by dispersion.

### 2.4.2 Removal of Oil from Glass Surface Method

The oil removal study was conducted using a glass slide [46]. The glass slide was covered uniformly with 100  $\mu\text{L}$  of heavy oil. The contaminated part of the glass slide was submerged in the test solution for 1 min before being dipped in distilled water to remove any excess test solution. The glass slide was then dried for 30 min at 40  $^\circ\text{C}$  in an air-forced oven and weighed. Distilled water was used as a control. The percentage of oil removal was calculated using Equation 6,

$$\text{Oil removal (\%)} = \frac{M_c - M_w}{M_c - M_i} \times 100 \quad (6)$$

where  $M_c$  is the mass of the glass slide contaminated,  $M_w$  is the mass of the glass slide after washing and drying, and  $M_i$  is the initial mass of the glass slide. Figure 2 shows an example of oil removal from the glass surface.

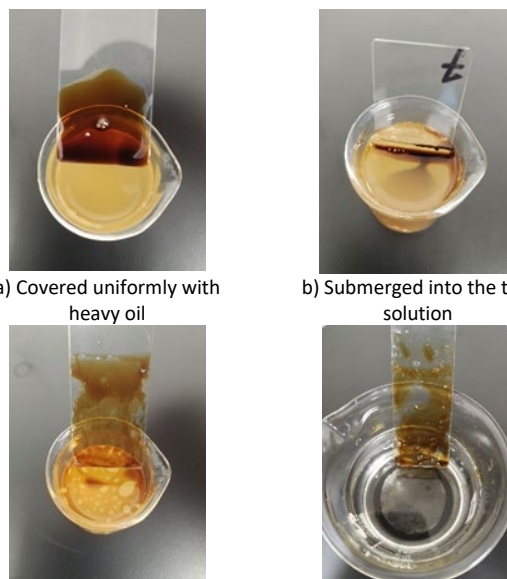


Figure 2 Method of removing oil from glass surface

### 3.0 RESULTS AND DISCUSSION

#### 3.1 Functional Groups and Chemical Structure of Rhamnolipid Biosurfactant

##### 3.1.1 Fourier Transform Infrared (FTIR) Spectra

The functional groups and type of bond of the rhamnolipid were examined by FTIR analysis (Figure 3). The broad peak at 3186.15–3194.19  $\text{cm}^{-1}$  confirmed the presence of  $\text{OH}$  stretching vibrations from hydroxyl groups, and the peak at 3027.57–3035.64  $\text{cm}^{-1}$  confirmed the presence of the  $\text{C-H}$  stretch of the  $\text{CH}_2$  and  $\text{CH}_3$  groups of aliphatic chains. The peak at 1625.45–1654.17  $\text{cm}^{-1}$  shows the  $\text{C=O}$  in  $\text{COOH}$ , and the stretching vibrations reveal the presence of ester carbonyl groups. A peak at 1402.46–1408.77  $\text{cm}^{-1}$  confirmed the presence of  $\text{C-O}$ , and the deformation vibrations indicate the ester carbonyl group of glycolipid extract. Meanwhile, the peak at 1042.08–1045.57  $\text{cm}^{-1}$  indicates  $\text{C-O-C}$  bonding characteristic of the glycosidic bond, indicating stretching in rhamnose. In addition, the peak at 604.67–606.60  $\text{cm}^{-1}$  is the stretching vibration of the  $(\text{CH}_2)_n$  group, showing the presence of di-rhamnolipid in the mixture. These results corresponded to the spectral bands observed in a previous investigation (Table 1). As a result of the analysis from the FTIR spectrum, these distinct adsorption bands show that rhamnolipid R90 (90% purity) contains chemical structures that are identical to those of rhamnolipids from previous studies [14], [20], [36], which contained rhamnose rings and long hydrocarbon chains as their primary structural components. In addition, the rhamnolipids are classified as belonging to the glycolipid group, composed of aliphatic acids and ester compounds.

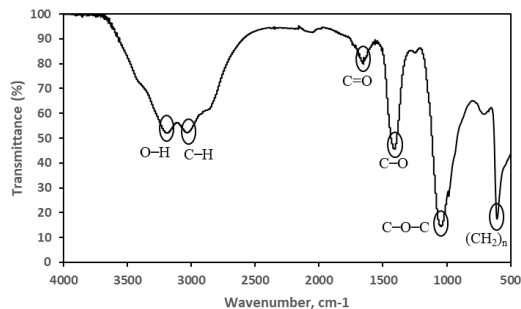


Figure 3 FTIR spectra of rhamnolipid biosurfactant

Table 1 FTIR spectra of rhamnolipid biosurfactant

Chemical Bond / Functional Group	Wavenumber, $\text{cm}^{-1}$ (this study)	Wavenumber, $\text{cm}^{-1}$ (from literature)
O-H stretch, hydroxyl group stretching of polysaccharides and carboxylic acids.	3186.15–3194.19	3278 [20], 3427 [36], [47], 3599.81 [14]
C-H stretch of $\text{CH}_2$ and $\text{CH}_3$ groups of aliphatic chains.	3027.57–3035.64	2856–2928 [48], 2874–3024 [36], 2924.49 [14]
C=O in $\text{COOH}$ , stretching associated with ester carbonyl groups.	1625.45–1654.17	1637 [20], 1732.04 [14], 1754 [36]

Chemical Bond / Functional Group	Wavenumber, $\text{cm}^{-1}$ (this study)	Wavenumber, $\text{cm}^{-1}$ (from literature)
C-O, deformation associated with ester carbonyl group of glycolipid extract.	1402.46–1408.77	1000–1300 [49], 1281 [50], 1458.42 [14]
C-O-C characteristic of the glycosidic bond, indicating stretching in rhamnose.	1042.08–1045.57	1040 [50], 1047 [48], 1144 [36]
$(\text{CH}_2)_n$ group.	604.67–606.60	740 [36], 834 [47]

##### 3.1.2 $^1\text{H}$ Nuclear Magnetic Resonance (NMR) and $^{13}\text{C}$ NMR Spectra

$^1\text{H}$  NMR and  $^{13}\text{C}$  NMR spectra were used to identify the structural properties of the rhamnolipid mixture (Figure 4). A chemical shift ( $\delta$ ) in the  $^1\text{H}$  NMR spectrum at 0.92 ppm revealed the presence of a  $\text{CH}_3$  group on  $\beta$  hydroxyl fatty acids. A chemical shift of 1.14 ppm indicated the presence of a  $\text{CH}_3$  group on a rhamnose moiety. The presence of  $-(\text{CH}_2)_n-$  on the aliphatic lipid chain was indicated by the shift at 1.313 ppm. The shift at 1.894 ppm for  $\text{C}_5/\text{C}_6$  (pentose or hexose) corresponds to sugar moieties. Chemical shifts at 2.175 ppm showed  $-(\text{CH}_2)-$  groups near carboxylic acid and ester groups. A chemical shift was found at 2.425 ppm for  $-\text{CH}(\text{O})-\text{CH}_2\text{COO}$  due to the  $\beta$ -hydroxy fatty acid chain. The presence of  $-\text{CH-OH}$  and  $-\text{COO-CH-}$  in the rhamnose moiety was shown by the signals at 3.585 and 5.363 ppm.

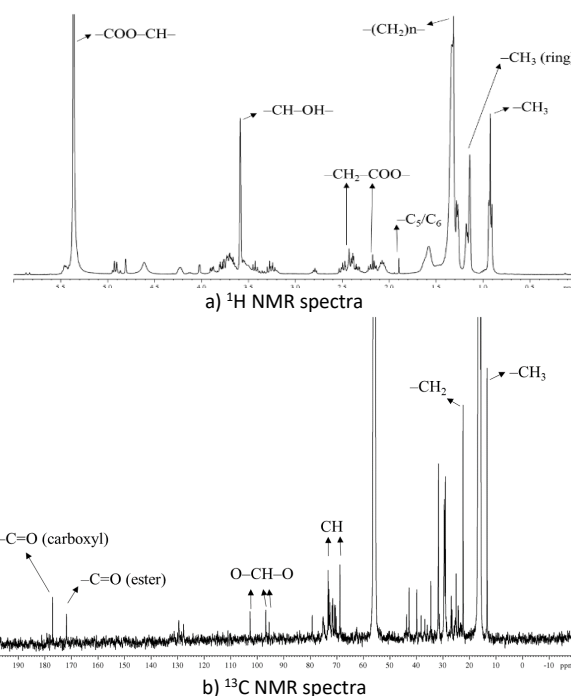


Figure 4 a)  $^1\text{H}$  NMR and b)  $^{13}\text{C}$  NMR spectra of the rhamnolipid biosurfactant

The resonance signals for lipids were observed in the  $^{13}\text{C}$  NMR spectra at 13.336 ppm ( $\text{CH}_3$ ), 22.386 ppm ( $\text{CH}_2$ ), and 68.781–73.248 ppm ( $\text{CH}$ ). The presence of  $\text{O-CH-O}$  was indicated by signals at 95.536, 96.728, and 102.655 ppm. In addition,  $-\text{C=O}$  (ester) and  $-\text{C=O}$  (carboxylic) group signals were observed at

171.810 and 177.052 ppm, respectively. From this characterization study, it can be concluded that the rhamnolipid contained hydroxy fatty acid chains and rhamnose moieties, consistent with previous studies (Table 2 and Table 3).

**Table 2**  $^1\text{H}$  NMR chemical shift data for rhamnolipid biosurfactant

Chemical Structure	Peak, ppm (this study)	Peak, ppm (from literature)
$-\text{CH}_3$ ( $\beta$ -hydroxy fatty acids)	0.920	0.85 [42], 0.85–0.88 [20], 0.86–0.89 [14]
$-\text{CH}_3$ (rhamnose moiety)	1.140	1.18–1.20 [35], 1.25 [20], 1.2612 [14]
$-(\text{CH}_2)_n-$ (aliphatic lipid chain)	1.313	1.24 [21], 1.29 [42], 1.33 [20]
$\text{C}_5/\text{C}_6$ (pentose or hexose) corresponding to sugar moieties	1.894	1.4–1.9 [42]
$-(\text{CH}_2)-$ (carboxylic acid and ester group)	2.175	1.97–2.56 [20], 2.23–2.40 [42], 2.33–2.52 [21]
$-\text{CH}(\text{O})-\text{CH}_2\text{COO}$ ( $\beta$ -hydroxy fatty acids)	2.425	2.5396 [14], 2.545 [47], 2.59 [35]
$-\text{CH}-\text{OH}$ (rhamnose moiety)	3.585	3.335 [47], 3.51–3.69 [20], 3.63 [35]
$-\text{COO}-\text{CH}-$ (rhamnose moiety)	5.363	5.24–5.35 [20], 5.27 [35], 5.3 [42]

**Table 3**  $^{13}\text{C}$  NMR chemical shift data for rhamnolipid biosurfactant

Chemical Structure	Peak, ppm (this study)	Peak, ppm (from literature)
$-\text{CH}_3$ (lipids)	13.336	13.7 [51], 14.1792 [14], 14.2–17.7 [20]
$-\text{CH}_2$ (lipids)	22.386	22.4–43.4 [20], 22.5–32.7 [51], 22.7032–31.8277 [14]
$-\text{CH}$	68.781–73.248	73.4–75.4 [20]
$\text{O}-\text{CH}-\text{O}$	95.536, 96.728, 102.655	93.9, 95.9, 102.9 [20]
$-\text{C}=\text{O}$ (ester)	171.810	171.5 [51], 171.5475 [14], 177.7 [20]
$-\text{C}=\text{O}$ (carboxyl)	177.052	172.4 [20], 173.6 [51], 173.8072 [14]

## 3.2 Stability of Rhamnolipid Solution

### 3.2.1 Surface Tension Behavior at Different Temperatures

As shown in Figure 5, the CMC was determined using the surface tension vs. rhamnolipid concentration plot, and all the calculated values are shown in Table 4. The surface tension of the rhamnolipid mixture was measured every 24 h, as shown in Figure 6. The surface tension was initially close to that of pure water (72 mN/m); the surface tension then decreased significantly when the rhamnolipid concentration increased, resulting in CMC values of 42–60 mg/L and 35–55 mg/L at 24 and 48 h, respectively. However, the surface tension increases at

higher concentrations at some points, as shown in Figure 6a. This effect could be due to the diluted rhamnolipids needing more than 24 h to stabilize. After 72 and 96 h, the CMC values increase at higher concentrations. This observation could be related to decreasing stability of the rhamnolipid solution with increased time. The lowest surface tension and CMC were achieved at 48 h (44 mN/m and 35 mg/L) at 55 °C.

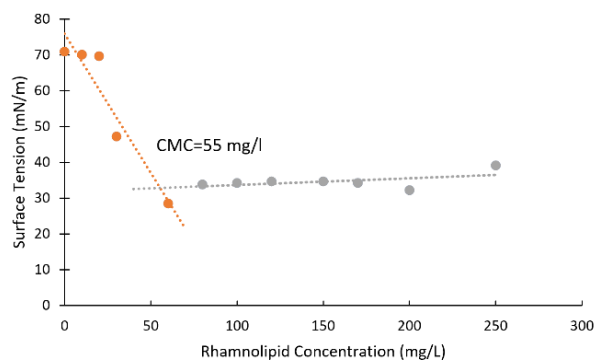


**Figure 5** Determination of the critical micellar concentration (CMC) (48 h, 25°C)

**Table 4** CMCs at 24, 48, 72, and 96 h at different temperature

Temperature °C	CMC (mg/L)			
	24 h	48 h	72 h	96 h
25	60	55	58	95
30	55	49	55	90
35	52	38	54	105
40	50	50	71	125
45	45	45	72	107
50	51	42	70	155
55	45	35	71	134
60	42	41	75	150

As the system temperature increased, the CMC of rhamnolipids at 24, 48, and 72 h initially declined and then increased, as illustrated in Figure 7. These findings are consistent with prior studies [29], [44], [52]–[54]. At first, the CMC reduces with increased temperature, decreasing the hydration of the hydrophilic rhamnose group, which promotes micellization. Then, when the temperature rose significantly, the water molecules near the hydrophobic groups tended to break down, interfering with the micellization process [44]. As a result, the initiation of the micellization process tends to intensify at higher concentrations. If the temperature continued to rise after the CMC had reached a minimum value, the CMC increased again with a further increase in temperature [44].

As shown in Figure 8, the surface tension at the CMC point decreased as the temperature increased, and it almost stabilized after 55 °C. A significant decrease was observed between 72 and 96 h. This phenomenon most likely occurred because of the breakdown of the hydrogen bonds within the water and the rhamnolipid molecules at higher temperatures [44], [52].

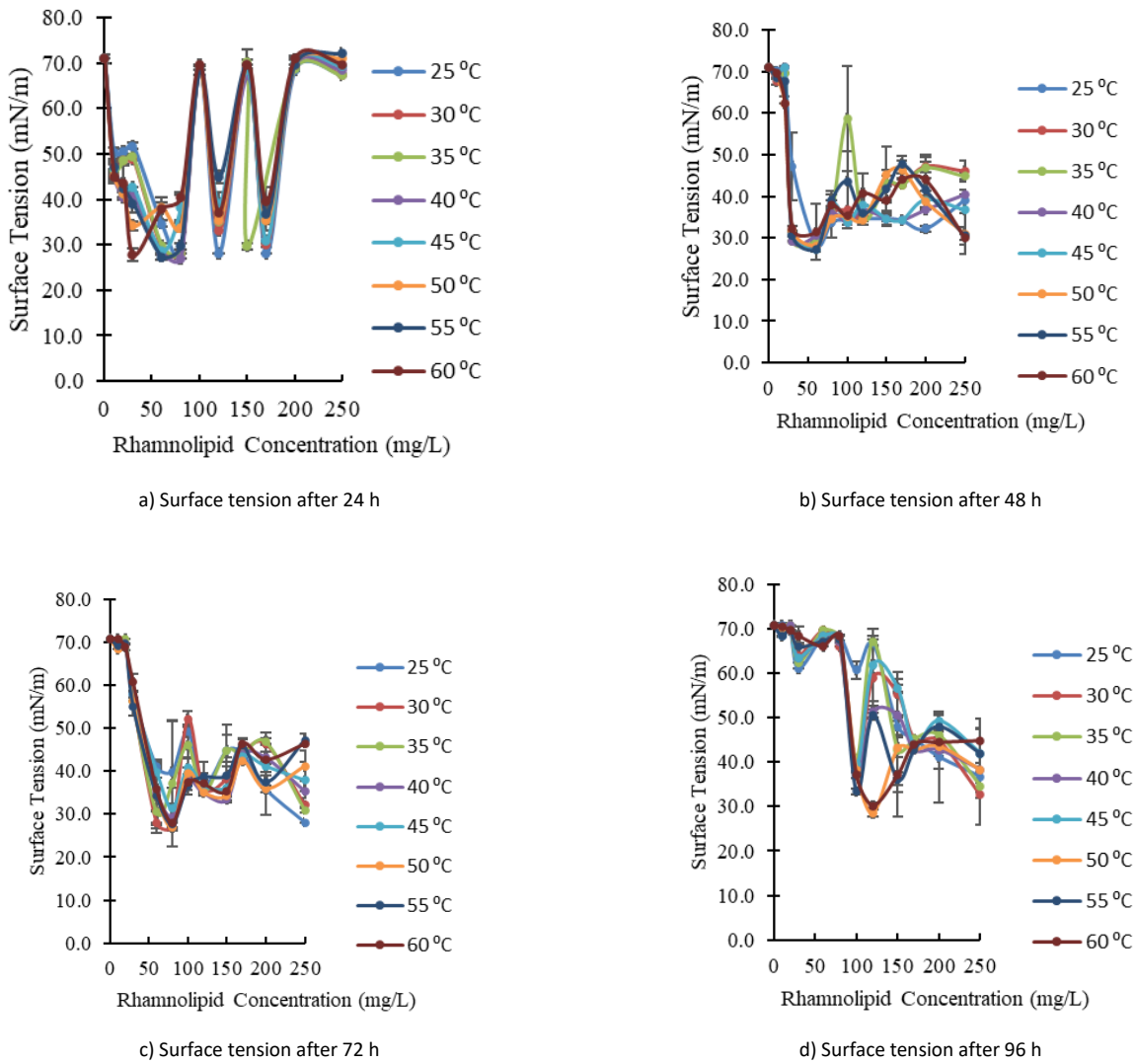


Figure 6 Variation of surface tension in aqueous solution at different times: (a) 24 h, (b) 48 h, (c) 72 h, and (d) 96 h and temperatures (25–60 °C)

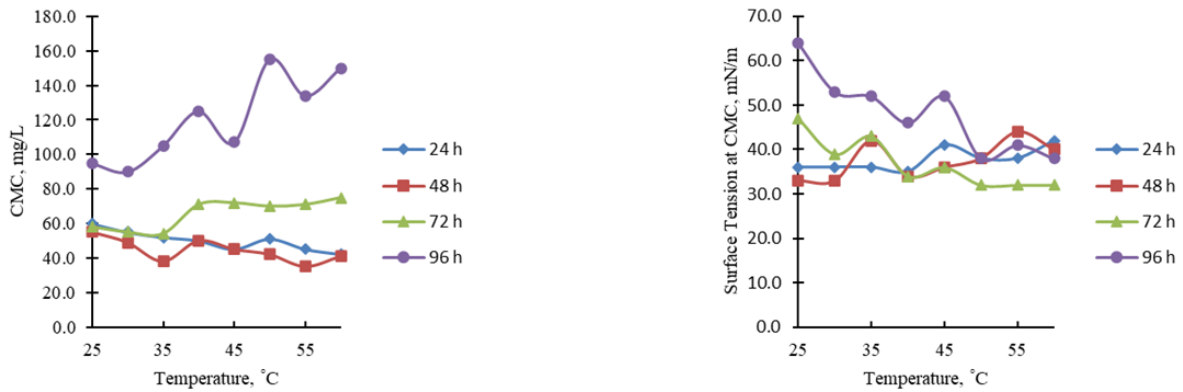


Figure 7 The variation of CMC with time at different temperatures

Figure 8 The variation in surface tension at the CMC with time at different temperatures

### 3.2.2 Micellization Properties at Different Temperatures

Table 5 shows the thermodynamic parameters for the rhamnolipid mixture at various times. The thermodynamic parameters revealed a tendency toward micellization in almost all of the solutions [55]. In addition, the thermodynamic analyses of the surfactant solutions suggest a deterministic technique for controlling the physicochemical properties of surfactant dosage formulations [30]. The experimental results reveal that the  $\Delta G_m^\circ$  decreases with increasing temperature from 24 to 72 h (298–333 K) and then increases drastically after 96 h (298–333 K). The solution was stable for 24 to 72 h.

The negative values of  $\Delta G_m^\circ$  revealed the stability of the rhamnolipid solution. A more negative  $\Delta G_m^\circ$  value indicates that the driving force for interactions increases substantially, making micellization thermodynamically more favorable [56]. The negative values of  $\Delta G_m^\circ$  are mostly related to positive entropy values ( $\Delta S_m^\circ$ ), particularly at low temperatures. These findings are consistent with prior studies, which indicated that

micellization is an entropy-driven process [44]. The negative values for  $\Delta G_m^\circ$  at all temperatures indicate that surfactant self-assembly occurs spontaneously [24], [41]. The value of  $\Delta G_m^\circ$  depends on the magnitude of the changes in  $\Delta H_m^\circ$  and  $\Delta S_m^\circ$  (see Equation 3). Additionally, the  $\Delta G_m^\circ$  value depends on the surfactant concentration. It is hypothesized that raising the surfactant concentration increases the surface free energy, in turn increasing the rate of the micellization process [57].

The negative value of  $\Delta H_m^\circ$  indicates that the micellization process was exothermic due to the lower activation energy resulting from the presence of rhamnolipids [58]. The value of  $\Delta H_m^\circ$  increased with temperature, indicating that hydrophobic interactions became stronger as the temperature increased due to the higher degree of hydration in the hydrophilic groups. The strong interaction could be due to the rising degree of electrostatic repulsion, which affects the dehydration of polar groups [59].

**Table 5** Temperature, CMC,  $X_{CMC}$ , and thermodynamic parameters for rhamnolipid biosurfactant with time

Time	Temp (K)	CMC (mM)	$X_{CMC}$	$\Delta G_m^\circ$ (kJmol <sup>-1</sup> )	$\Delta H_m^\circ$ (kJmol <sup>-1</sup> )	$\Delta S_m^\circ$ (kJmol <sup>-1</sup> K <sup>-1</sup> )
24 h	298	0.0922	0.0017	-15858.0111	-13826.8199	6.8161
	303	0.0845	0.0015	-16073.6010	-14058.7195	6.7613
	308	0.0799	0.0014	-16212.5751	-14290.6190	6.4495
	313	0.0768	0.0014	-16309.7531	-14522.5186	5.9974
	318	0.0691	0.0012	-16570.8070	-14754.4182	6.0953
	323	0.0784	0.0014	-16260.6877	-14986.3178	4.2764
	328	0.0691	0.0012	-16570.8070	-15218.2174	4.5389
	333	0.0645	0.0012	-16741.7521	-15450.1170	4.3343
48 h	298	0.0845	0.0015	-16073.6010	-10055.4611	20.1951
	303	0.0753	0.0014	-16359.8097	-10224.1084	20.5896
	308	0.0584	0.0011	-16989.7310	-10392.7557	22.1375
	313	0.0768	0.0014	-16309.7531	-10561.4030	19.2898
	318	0.0691	0.0012	-16570.8070	-10730.0503	19.5999
	323	0.0645	0.0012	-16741.7521	-10898.6976	19.6076
	328	0.0538	0.0010	-17193.4941	-11067.3449	20.5575
	333	0.0630	0.0011	-16801.4591	-11235.9922	18.6761
72 h	298	0.0891	0.0016	-15942.0097	-17809.5151	-6.2668
	303	0.0845	0.0015	-16073.6010	-18108.2119	-6.8276
	308	0.0830	0.0015	-16119.0651	-18406.9086	-7.6773
	313	0.1091	0.0020	-15440.9232	-18705.6053	-10.9553
	318	0.1106	0.0020	-15406.2692	-19004.3021	-12.0739
	323	0.1076	0.0019	-15476.0687	-19302.9988	-12.8420
	328	0.1091	0.0020	-15440.9232	-19601.6955	-13.9623
	333	0.1152	0.0021	-15305.1237	-19900.3922	-15.4204
96 h	298	0.1460	0.0026	-14719.4182	-14048.3712	2.2518
	303	0.1383	0.0025	-14853.3817	-14283.9871	1.9107
	308	0.1613	0.0029	-14471.4393	-14519.6030	-0.1616
	313	0.1921	0.0035	-14039.4403	-14755.2189	-2.4019
	318	0.1644	0.0030	-14424.6885	-14990.8347	-1.8998
	323	0.2382	0.0043	-13506.4543	-15226.4506	-5.7718
	328	0.2059	0.0037	-13867.1741	-15462.0665	-5.3520
	333	0.2305	0.0042	-13587.6983	-15697.6823	-7.0805

### 3.3 Potential Application of Rhamnolipids for Oil Degradation

From the characterization, the rhamnolipid mixture effectively reduced the surface tension and CMC in higher concentrations and temperatures after 24 h. This increase in concentration and temperature accelerates the micellization process [44]. These low CMC values were required to reduce the amount of cleaning

product used during the cleaning process, form micelles, and remove dirt [26]. The ODT measures the diameter of the clear area that appears after a cleaning solution is added to a thin layer of oil in water to estimate its dispersion capacity [46]. Table 6 shows the result of the ODTs of rhamnolipid solutions with varying concentrations. The dispersion was 0 when water was used as a control. The dispersion was also 0 at 0.01% w/v

rhamnolipid concentration. The dispersion was  $90 \pm 0.00$  mm at 0.1% w/v rhamnolipid concentration and  $240 \pm 0.00$  mm at 1% w/v rhamnolipid concentration. A clear area with a larger diameter indicates stronger surface action on oil degradation [46].

The effectiveness of a cleaning product can be measured by its ability to remove oil from a glass surface [46]. Figure 9 illustrates oil removal from a glass surface by different concentrations of the rhamnolipid mixture. The removal of oil from each concentration is shown in Figures 9a (control), 9b (0.01% w/v), 9c (0.1% w/v), and 9d (1% w/v). The most effective oil removal occurred at 1% w/v concentration ( $51.18\% \pm 0.53\%$ ).

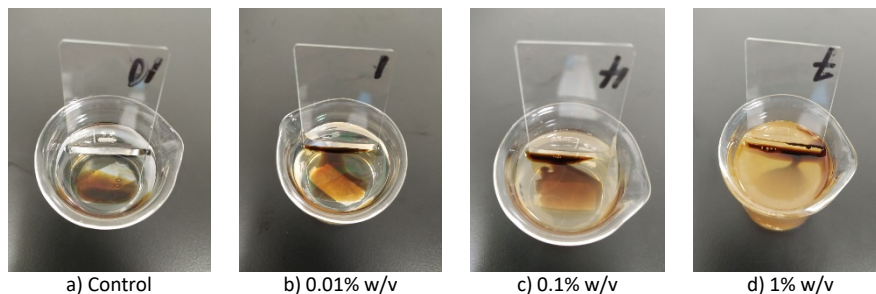


Figure 9 Removal of oil from a glass surface by different concentrations of rhamnolipids

#### 4.0 CONCLUSION

This study clarified the presence of functional groups and the chemical structure of rhamnolipids, which agreed with most previous studies. The micellization process of the rhamnolipids was spontaneous and exothermic. Increased temperature decreased hydration of the hydrophilic rhamnose groups, promoting micellization at lower concentrations after 24 to 72 h. After 96 h, the stability of rhamnolipid decreased. Thus, the recommended minimum amount of rhamnolipid that should be included in the oil degreaser formulation is 0.1% w/v, which is very low. This study explained the factors influencing oil degreasing efficacy, including temperature and concentration.

#### Acknowledgments

This work was sponsored by the Universiti Teknologi Malaysia Fundamental Research (UTMFR) program [grant number Q.J130000.2509.21H54].

#### References

- [1] B. Doshi, M. Sillanpää, and S. Kalliola, 2018, "A review of bio-based materials for oil spill treatment," *Water Research*, 135: 262–277, doi: 10.1016/j.watres.2018.02.034.
- [2] S. Farag, N. A. Soliman, and Y. R. Abdel-fattah, 2018, "Statistical optimization of crude oil bio-degradation by a local marine bacterium isolate *Pseudomonas sp.* sp48," *Journal of Genetic Engineering and Biotechnology*, 16(2): 409–420, doi: 10.1016/j.jgeb.2018.01.001.
- [3] I. J. B. Durval et al., 2019 "Application of *Bacillus cereus* UCP 1615 biosurfactant for increase dispersion and removal of motor oil from contaminated sea water," *Chemical Engineering Transactions*, 74(January): 319–324, , doi: 10.3303/CET1974054.

Table 6 Oil degradation ability on different rhamnolipid concentrations

Rhamnolipid Concentration (% w/v)	ODT, mm	Removal of Oil, %
Control	ND	12.86±0.90
0.01	ND	26.89±0.91
0.1	90±0.00	44.52±0.86
1	240±0.00	51.18±0.53

ND = not dispersed

- [4] J. M. Luna, B. G. A. Lima, M. I. S. Pinto, P. P. F. Brasileiro, R. D. Rufino, and L. A. Sarubbo, 2017, "Application of *Candida sphaerica* biosurfactant for enhanced removal of motor oil from contaminated sand and seawater," *Chemical Engineering Transactions*, 57: 565–570, doi: 10.3303/CET1757095.
- [5] P. Parthipan, E. Preetham, L. L. Machuca, P. K. S. M. Rahman, K. Murugan, and A. Rajasekar, 2017, "Biosurfactant and degradative enzymes mediated crude oil degradation by bacterium *Bacillus subtilis* A1," *Frontier in Microbiology*, 8(February): 1–14, doi: 10.3389/fmicb.2017.00193.
- [6] J. Shi, Y. Chen, X. Liu, and D. Li, 2021, "Rhamnolipid production from waste cooking oil using newly isolated halotolerant *Pseudomonas aeruginosa* M4," *Journal of Cleaner Production*. 278: 123879, doi: 10.1016/j.jclepro.2020.123879.
- [7] C. E. Drakontis and S. Amin, 2020, "Biosurfactants: Formulations, properties, and applications," *Current Opinion in Colloid and Interface Science*, 48: 77–90, Doi: 10.1016/j.cocis.2020.03.013.
- [8] S. Varjani et al., 2021, "Bio-based rhamnolipids production and recovery from waste streams: Status and perspectives," *Bioresour Technol*. 319: 124213. doi: 10.1016/j.biortech.2020.124213.
- [9] S. Vijayakumar and V. Saravanan, 2015, "Biosurfactants-types, sources and applications," *Research Journal of Microbiology*. 10(5): 181–192, doi: 10.3923/jm.2015.181.192.
- [10] E. O. Fenibo, G. N. Ijoma, R. Selvarajan, and C. B. Chikere, 2019, "Microbial surfactants: The next generation multifunctional biomolecules for applications in the petroleum industry and its associated environmental remediation," *Microorganisms*, 7(11): 1–29, doi: 10.3390/microorganisms7110581.
- [11] H. R. Ahmadi-Ashtiani et al., 2020, "Microbial biosurfactants as key multifunctional ingredients for sustainable cosmetics," *Cosmetics*, 7(2): 1–35, doi: 10.3390/COSMETICS7020046.
- [12] R. Jahan, A. M. Bodratti, M. Tsianou, and P. Alexandridis, 2020, "Biosurfactants, natural alternatives to synthetic surfactants: Physicochemical properties and applications," *Advances in Colloid and Interface Science*. 275: 102061, doi: 10.1016/j.cis.2019.102061.
- [13] G. S. Shreve and R. Makula, 2019 "Characterization of a new rhamnolipid biosurfactant complex from *Pseudomonas* isolate DYNA270," *Biomolecules*, 9(12): 1–11, doi: 10.3390/biom9120885.
- [14] S. Haloi, S. Sarmah, S. B. Gogoi, and T. Medhi, 2020 "Characterization of *Pseudomonas sp.* TMB2 produced rhamnolipids for ex-situ microbial enhanced oil recovery," *Biotech*, 10(3): 1–17, , doi: 10.1007/s13205-020-2094-9.



- [15] Q. Helmy, S. Gustiani, and A. T. Mustikawati, 2020, "Application of rhamnolipid biosurfactant for bio-detergent formulation," *IOP Conference Series: Materials Science and Engineering* 823(1): 012014. doi: 10.1088/1757-899X/823/1/012014.
- [16] A. M. Abdel-Mawgoud, M. M. Aboulwafa, and N. A. H. Hassouna, 2009, "Characterization of rhamnolipid produced by *Pseudomonas aeruginosa* isolate Bs20," *Applied Biochemistry and Biotechnology*, 157(2): 329–345, doi: 10.1007/s12010-008-8285-1.
- [17] H. Amani, 2015, "Study of enhanced oil recovery by rhamnolipids in a homogeneous 2D micromodel," *Journal of Petroleum Science and Engineering*. 128: 212–219, doi: 10.1016/j.petrol.2015.02.030.
- [18] S. G. V. A. O. Costa, M. Nitschke, F. Lépine, E. Déziel, and J. Contiero, 2010, "Structure, properties and applications of rhamnolipids produced by *Pseudomonas aeruginosa* L2-1 from cassava wastewater," *Process Biochemistry* 45(9): 1511–1516, doi: 10.1016/j.procbio.2010.05.033.
- [19] M. Hořková et al., 2015 "Structural and physicochemical characterization of rhamnolipids produced by *Acinetobacter calcoaceticus*, *Enterobacter asburiae* and *Pseudomonas aeruginosa* in single strain and mixed cultures," *Journal of Biotechnology*. 193: 45–51, doi: 10.1016/j.jbiotec.2014.11.014.
- [20] A. S. Pathania and A. K. Jana, 2020, "Improvement in production of rhamnolipids using fried oil with hydrophilic co-substrate by indigenous *Pseudomonas aeruginosa* NJ2 and characterizations," *Applied Biochemistry and Biotechnology*, 191: 1223–1246. doi: <https://doi.org/10.1007/s12010-019-03221-9> Improvement.
- [21] S. Sana, S. Datta, D. Biswas, and M. Bhattacharya, 2017, "Production kinetics of rhamnolipid using fish fat: A step towards environmental hazard control of sewage," *Environmental Technology and Innovation*. 8: 299–308, doi: 10.1016/j.eti.2017.07.004.
- [22] C. Zheng, M. Wang, Y. Wang, and Z. Huang. 2012. "Optimization of biosurfactant-mediated oil extraction from oil sludge," *Bioresource Technology*. 110: 338–342, Doi: 10.1016/j.biortech.2012.01.073.
- [23] A. T. Phung, Q. H. Nguyen, H. Q. Duong, and H. H. Cao, 2020. "Study of wetting on the non-image area of offset printing plates by an alternative iso-propyl alcohol-free fountain solution," *ASEAN Engineering Journal*. 10(2):50–57, Doi: 10.11113/aej.v10.16596.
- [24] J. C. Roy, S. Das, and M. N. Islam, 2019. "Influence of kosmotropes and chaotropes on the krafft temperature and critical micelle concentration of tetradecyltrimethylammonium bromide in aqueous solution," *Journal of Solution Chemistry*. 758–773, doi: 10.1007/s10953-019-00879-x.
- [25] K. C. Cheng, Z. S. Khoo, N. W. Lo, W. J. Tan, and N. G. Chemmangattavalappil, 2020, "Design and performance optimisation of detergent product containing binary mixture of anionic-nonionic surfactants," *Heliyon*, 6(5) doi: 10.1016/j.heliyon.2020.e03861.
- [26] C. B. B. Farias, R. C. F. Soares da Silva, F. C. G. Almeida, V. A. Santos, and L. A. Sarubbo, 2021, "Removal of heavy oil from contaminated surfaces with a detergent formulation containing biosurfactants produced by *Pseudomonas spp.*," *PeerJ*, 9: 1–27, doi: 10.7717/peerj.12518.
- [27] A. Pradhan and A. Bhattacharyya, 2017, "Quest for an eco-friendly alternative surfactant: Surface and foam characteristics of natural surfactants," *Journal of Cleaner Production*. 150: 127–134, doi: 10.1016/j.jclepro.2017.03.013.
- [28] P. Shi, H. Zhang, L. Lin, C. Song, Q. Chen, and Z. Li, 2019, "Molecular dynamics simulation of four typical surfactants in aqueous solution," *RSC Advances*. 9(6):3224–3231, doi: 10.1039/c8ra09670h.
- [29] A. Moradi and A. Bagheri, 2022, "Effect of a biosurfactant on micellar behavior of cationic surfactants in aqueous solution," *Journal of Solution Chemistry*. 51: 499-516. doi: 10.1007/s10953-022-01149-z.
- [30] N. Pal, K. Samanta, and A. Mandal, 2019, "A novel family of non-ionic gemini surfactants derived from sunflower oil: Synthesis, characterization and physicochemical evaluation," *Journal of Molecular Liquids*. 275: 638–653, doi: 10.1016/j.molliq.2018.11.111.
- [31] G. D. Noudeh, M. Housaindokht, and B. S. F. Bazzaz, 2007, "The effect of temperature on thermodynamic parameters of micellization of some surfactants," *Journal of Applied Sciences*, 7(1): 47–52, doi: 10.3923/jas.2007.47.52.
- [32] J. Oremusová et al., 2019, "Effect of molecular composition of head group and temperature on micellar properties of ionic surfactants with C12 alkyl chain," *Molecules*, 24(3): 651, doi: 10.3390/molecules24030651.
- [33] Y. Li, R. Lian, X. Wang, and Y. Liu, 2020 "The aggregation behavior of fluorinated surfactant in an ionic liquid," *Colloid and Polymer Science*. 298(8):1013–1021, doi: 10.1007/s00396-020-04650-3.
- [34] M. K. Bafghi and M. H. Fazaelpoor, 2012, "Application of rhamnolipid in the formulation of a detergent," *Journal of Surfactants and Detergents*. 15(6):679–684, doi: 10.1007/s11743-012-1386-4.
- [35] J. V. Jadhav, P. Anbu, S. Yadav, A. P. Pratap, and S. B. Kale, 2019, "Sunflower acid oil-based production of rhamnolipid using *Pseudomonas aeruginosa* and its application in liquid detergents," *Journal of Surfactants and Detergents* 22(3): 463–476, doi: 10.1002/jsde.12255.
- [36] M. Aghajani, A. Rahimpour, H. Amani, and M. J. Taherzadeh, 2018, "Rhamnolipid as new bio-agent for cleaning of ultrafiltration membrane fouled by whey," *Engineering in Life Sciences*. 18(5): 272–280, doi: 10.1002/elsc.201700070.
- [37] X. Long, Q. Meng, and G. Zhang, 2014, "Application of biosurfactant rhamnolipid for cleaning of UF membranes," *Journal of Membrane Science*, 457: 113–119, doi: 10.1016/j.memsci.2014.01.044.
- [38] R. Turbekar, N. Malik, D. Dey, and D. Thakare, 2014, "Development of rhamnolipid based white board cleaner," *International Journal of Applied Sciences and Biotechnology*. 2(4): 570–573, doi: 10.3126/ijasbt.v2i4.11589.
- [39] T. G. Ambaye, M. Vaccari, S. Prasad, and S. Rtimi, 2021, "Preparation, characterization and application of biosurfactant in various industries: A critical review on progress, challenges and perspectives," *Environmental Technology and Innovation*. 24: 102090, doi: 10.1016/j.eti.2021.102090.
- [40] A. A. Jimoh and J. Lin, 2019, "Biosurfactant: A new frontier for greener technology and environmental sustainability," *Ecotoxicology and Environmental Safety*. 184(august): 109607, doi: 10.1016/j.ecoenv.2019.109607.
- [41] M. A. Saad, N. H. Abdurahman, and R. M. Yunus, 2020, "Eco-friendly surfactant to demulsification water in oil emulsion: synthesis, characterization and application," *Chemical Data Collections*, 30, doi: 10.1016/j.cdc.2020.100582.
- [42] S. Ratna and R. Kumar, 2022, "Production of di-rhamnolipid with simultaneous distillery wastewater degradation and detoxification by newly isolated *Pseudomonas aeruginosa* SRRBL1," *Journal of Cleaner Production*, 336(August): 130429, doi: 10.1016/j.jclepro.2022.130429.
- [43] R. Kumar and A. J. Das, 2018, "Rhamnolipid biosurfactant. Recent trends in production and application," *Springer Nat. Singapore Pte Ltd*, 1–141, doi: 10.1007/9789811312892.
- [44] E. Mohajeri and G. D. Noudeh, 2012, "Effect of temperature on the critical micelle concentration and micellization thermodynamic of nonionic surfactants: Polyoxyethylene sorbitan fatty acid esters," *E-Journal of Chemistry*. v9(4): 2268–2274, doi: 10.1155/2012/961739.
- [45] B. G. Freitas et al., 2016, "Formulation of a commercial biosurfactant for application as a dispersant of petroleum and by-products spilled in oceans," *Frontiers in Microbiology*, 7: 1–9 doi: 10.3389/fmicb.2016.01646.
- [46] N. M. P. R. e Silva, F. C. G. Almeida, F. C. P. R. e Silva, J. M. Luna, and L. A. Sarubbo, 2020, "Formulation of a biodegradable detergent for cleaning oily residues generated during industrial processes," *Journal of Surfactants and Detergents*. 23(6): 1111–1123, doi: 10.1002/jsde.12440.
- [47] T. A. A. Moussa, M. S. Mohamed, and N. Samak, 2014, "Production and characterization of di-rhamnolipid produced by *Pseudomonas aeruginosa* TMN," *Brazilian Journal of Chemical Engineering*. 31(3): 867–880 doi: 10.1590/0104-6632.20140314s00002473.
- [48] M. Ghorbani, M. Hosseini, G. Najafpour, and R. Hajimohammadi, 2021, "Synthesis and characterization of rhamnolipid biosurfactant produced by *Pseudomonas aeruginosa* PTCC 1340 for emulsification of oil sludge in oil storage tank," *Arabian Journal for Science and Engineering*. 47: 219–226, doi: 10.1007/s13369-021-05872-5.
- [49] S. Nalini and R. Parthasarathi, 2014, "Production and characterization of rhamnolipids produced by *Serratia rubidua* SNAU02 under solid-state fermentation and its application as biocontrol agent," *Bioresource Technology*. 173: 231–238, doi: 10.1016/j.biortech.2014.09.051.

- [50] R. Patowary, K. Patowary, M. C. Kalita, and S. Deka, 2016, "Utilization of paneer whey waste for cost-effective production of rhamnolipid biosurfactant," *Applied Biochemistry and Biotechnology*. 180(3):383–399, doi: 10.1007/s12010-016-2105-9.
- [51] N. Christova et al., 2013, "Chemical structure and in vitro antitumor activity of rhamnolipids from *Pseudomonas aeruginosa* BN10," *Applied Biochemistry and Biotechnology*. 170(3): 676–689, doi: 10.1007/s12010-013-0225-z.
- [52] O. Chidi and I. V. Adebayo, 2018 "Determination of critical micelle concentration and thermodynamic evaluations of micellization of GMS," *Modern Chemistry & Applications*. 6(2): 1000251 doi: 10.4172/2329-6798.1000251.
- [53] H. U. Kim and K. H. Lim, 2004, "A model on the temperature dependence of critical micelle concentration," *Colloids and Surfaces A: Physicochemical and Engineering Aspects*. 235(1-3): 121–128, doi: 10.1016/j.colsurfa.2003.12.019.
- [54] M. E. Mahmood and D. A. F. Al-koofee, 2013. "Effect of temperature changes on critical micelle concentration for tween series surfactant," *Global Journal of Science Frontier Research Chemistry*. 13(4): 1–7
- [55] N. A. Negm and S. M. Tawfik, 2014, "Characterization, surface properties and biological activity of some synthesized anionic surfactants," *Journal of Industrial and Engineering Chemistry*. 20(6): 4463–4472, doi: 10.1016/j.jiec.2014.02.018.
- [56] M. A. Rub, N. Azum, A. M. Asiri, H. A. Kashmery, S. Y. M. Alfaifi, and S. S. Alharthi, 2017, "Effect of sodium dodecylbenzenesulfonate on the association behavior of promethazine hydrochloride in aqueous/electrolyte solutions at different temperatures," *Journal of Solution Chemistry*. 46(4): 862–885, doi: 10.1007/s10953-017-0614-y.
- [57] M. Diana, Z. Anna, and J. Bronislaw, 2014, "Thermodynamic properties of rhamnolipid micellization and adsorption," *Colloids Surfaces B Biointerfaces*, 119: 22–29, doi: 10.1016/j.colsurfb.2014.04.020.
- [58] A. Ali, S. Uzair, S. Tasneem, and F. Nabi, 2014, "A thermodynamic study of lipid-surfactant interactions in non-aqueous media," *Journal of Solution Chemistry*. 43(11): 1817–1829, doi: 10.1007/s10953-014-0246-4.
- [59] N. Younas and M. A. Rashid, 2020, "Thermodynamic, spectroscopic and biological investigation of interaction of anionic surfactants with  $[\text{Cu}(\text{im})_6]\text{F}_2 \cdot 4\text{H}_2\text{O}$  complex in aqueous solution," *Colloids and Interface Science Communications*. 35(january): 100240, doi: 10.1016/j.colcom.2020.100240.